Clays and Clay Minerals, Vol. 40, No. 5, 593–599, 1992.

NATURAL AND SYNTHETIC COPPER PHYLLOSILICATES STUDIED BY XPS

CHRISTINE MOSSER
Centre de Géochimie de la Surface, CNRS, 1 rue Blessig, 67084 Strasbourg, France

AIMÉ MOSSER AND MICHELANGELO ROMEO
Institut de Physique et Chimie des Matériaux de Strasbourg
4 rue Blaise Pascal, 67070 Strasbourg Cedex, France

SABINE PETIT AND ALAIN DECARREAU
Laboratoire de Pétrologie de la Surface, URA 721 du CNRS, Université de Poitiers
40 Avenue du Recteur Pineau, 86022 Poitiers Cedex, France

Abstract—X-ray photoelectron spectroscopy (XPS) has been used to characterize the bonding state of Cu^{2+}, Si^{4+}, Al^{3+}, and O^{2-} ions in structural (octahedral and interlamellar) or adsorbed position in phyllosilicates. Five smectites, 5 kaolinites, and 1 chrysocolla with Cu(II) in known positions (octahedral, interlamellar, or surface adsorbed) have been investigated. Their spectra were compared with those of pure Cu metal and of pure Cu(I) and Cu(II) oxides.

The line for Cu $2p_{3/2}$ (binding energy of 935.4 eV) and well-defined shake-up lines (binding energy of about 943 eV) observed after 1 hr of X-ray irradiation are characteristic of Cu(II) in phyllosilicate octahedral sites. But due to the photoreduction effect, they show Cu(I) oxidation states (Cu $2p_{3/2}$, binding energy of 933.2 eV and near absence of shake-up lines) for the phyllosilicates with adsorbed Cu or in interlamellar positions. The kinetics of photoreduction distinguishes octahedral from interlamellar positions, and the latter from a surface adsorbed position. The enlargement of the FWHM (full width at half maximum) of XPS lines has been used to describe crystallochemical parameters linked to local ordering around the probe cations. Crystallization produces decreasing O 1s and Cu 2p (octahedral cation) line widths but has no effect on the Si 2p (tetrahedral cation) line width. The enlargement of FWHM for all ion lines of the lattice is linked to the nature (Cu > Mg > Al) and the number and amount of structural cations in the phyllosilicates.

Key Words—Chrysocolla, Cu, ESCA, Kaolinite, Smectite, XPS.

INTRODUCTION

X-ray photoelectron spectroscopy (XPS) is a useful spectroscopic tool for near-surface regions. A recent reassessment of electron escape depths in silica (Hochella and Carim, 1988) indicates that 95% of 1 keV electrons (the approximate kinetic energy of O 1s electrons excited with AlKα X-rays) comes from approximately the top 60 Å of the sample. Since the c-axis of phyllosilicates in an air-dry state is a maximum of 14 Å, XPS analysis of such material is a study of the bulk structure when the emitted electrons are collected perpendicular to the ab plane of these minerals.

It has been known since the early work of Siegbahn *et al.* (1967) that the exact position of photoelectron peaks can be indicative of the chemical and/or the structural environment of the analysed element, as well as its oxidation state. So the bonding state of elements can be characterised by XPS spectroscopy. Moreover, the chemical shift in the photoelectron binding energy depends on the electron density of an atom. Generally, the photoelectron binding energy decreases with increasing electron density (Huntress and Wilson, 1972; Stucki *et al.*, 1976; Seyama and Soma, 1985, 1988).

Hochella and Brown (1988) pointed out that the FWHM of the O 1s photopeak is proportional to the number of chemically distinct oxygen bonding environments in each silicate structure they studied. Peak position and FWHM seem then to be the two most interesting parameters giving information about the bonding of elements.

XPS was used here to study the localisation of Cu(II) in different synthetic and natural phyllosilicates. Therefore smectites, kaolinites, and chrysocolla with Cu(II) in known positions (surface adsorbed, octahedral, and interlamellar) were studied. Investigations were also undertaken to characterize the bonding state of Cu^{2+}, Si^{4+}, Al^{3+}, and O^{2-} ions in structural or adsorbed positions in phyllosilicates.

MATERIALS AND METHODS

Five smectites, 5 kaolinites, and 1 chrysocolla were studied and parts of their XPS spectra were compared

Table 1. Chemical composition of the studied phyllosilicates.

	SiO_2	Al_2O_3	MgO	Fe_2O_3	CuO	SrO	LOI
SMBF	52.6	23.7	0.7	3.4	2.9	2.6	11.4
SMCB	60.8	20.0	3.7	2.9	—	—	12.2
SMCUI	59.0	19.4	3.6	2.8	3.6	—	8.6
SMR3	54.8	—	24.7	—	5.5	—	15.0
SMMG	57.5	—	27.5	—	—	—	15.0
KPA3	49.3	33.5		2.1	1.0		13.9
KMRX	44.9	39.3	—	0.4	—	—	13.9
KCUAD	44.9	39.3	—	0.4	<0.1	—	13.9
KCUIO	35.5	15.0	—	—	35.5	—	14.0
KCU7	45.5	37.5			3.0		14.0
CHYSN	36.4	1.3	0.2	0.7	39.4	—	20.7

SMBF = natural aluminous smectite from Burkina Faso with Cu in octahedral position.

SMCB = natural aluminous smectite from Camp Berteau, Morocco.

SMCUI = Camp Berteau smectite with Cu in interlamellar position.

SMR3 = synthetic Cu smectite with Cu in octahedral position.

SMMG = synthetic Mg smectite with only Mg in octahedral position.

KPA3 = natural kaolinite from weathering profiles near Chapada Grande, Brazil with Cu in octahedral position.

KMRX = natural kaolinite from Montroux, Charentes Maritimes, France.

KCUAD = Cu-saturated kaolinite from Charentes Maritimes.

KCUIO = synthetic Cu kaolinite with Cu in octahedral position.

KCU7 = synthetic Cu kaolinite with Cu in octahedral position.

CHYSN = natural chrysocolla from Santa-Blandina, Brazil, with Cu in octahedral position.

CUIOD (not listed above) is the gel obtained by precipitation of Al and Cu nitrates and Na metasilicate. By hydrothermal treatment this gel is transformed into kaolinite. CUIOD has the same chemical composition as KCUIO.

with those of pure Cu metal and of pure Cu(I) and Cu(II) oxides, namely Cu_2O and CuO. The identities and chemical compositions of the phyllosilicates are given in Table 1. Reference data for typical XPS line positions are summarized in Table 2.

Smectite with Cu(II) in the interlamellar position and kaolinite with Cu(II) adsorbed on the surface were prepared in the following way. Montmorillonite from Camp Berteau (Morocco) and kaolinite from Montroux (France) were washed three times in 0.1 N $CuCl_2$ solution at pH 3.6, then repeatedly rinsed with water until the supernatant gave a negative $AgNO_3$ test for chloride.

Smectite and kaolinite with Cu(II) in octahedral positions and Mg-smectite were synthesized according to the procedures described by Decarreau (1985) and Petit (1990). The Cu(II) crystallographic positions in the different clays were determined by ESR and EXAFS spectroscopies, and by X-ray microanalysis (Creach, 1989; Mosser *et al.*, 1990a, 1990b).

XPS spectra were recorded on a CAMECA-RIBER NANOSCAN 50 apparatus equipped with an AlKα source and a MAC 2 analyser which was set at 1 eV energy resolution. The phyllosilicates were dispersed in distilled water by ultrasonic treatment. A drop of that dispersion was placed on a 2-cm disk of refractory vitreous carbon, air-dried, and analysed by XPS spectroscopy. Compensation for sample charging was made by setting the binding energies relative to the C 1s line at 284.6 eV. This carbon was present due to hydrocarbon contamination.

RESULTS AND DISCUSSION

XPS spectra of the minerals (smectite, kaolinite, chrysocolla) were compared with those of Cu metal, Cu_2O, and CuO (Figure 1). The charge-corrected Cu $2p_{3/2}$, O 1s and Si 2p peak positions and their FWHM are given in Table 2.

Structural and oxidation state effects

The Cu $2p_{3/2}$ binding energy differs between CuO (933.5 eV) and phyllosilicates (about 935.4 eV) because, even though Cu is in the same (II) oxidation state, the geometrical diposition of O around the Cu is not the same. In the phyllosilicates, Cu is in the center of a distorted octahedron (Creach, 1988; Mosser *et al.*, 1990a, 1990b), with the same interatomic distance of 1.95 Å between Cu and the 4 planar O, and a greater distance between Cu and the 2 apical O (2.41 Å for chrysocolla and 2.32 Å for synthetic Cu-smectite). For CuO the coordination of oxygen and copper is more properly described as 4-planar rather than as 4 + 2 distorted octahedral coordination, with Cu-O bond length of 1.95 Å to 1.96 Å for the four planar oxygens and 2.78 Å for the two distant O atoms (Asbrink and Norrby, 1970). An increase in binding energy with increasing interatomic bond lengths was also pointed out by Urch and Murphy (1974) and can be described as a structural effect.

Copper ions in CuO and Cu_2O are in similar chemical (Cu and O) environments with Cu-O bond lengths of 1.95 Å (Asbrink and Norrby, 1970) and 1.85 Å (Wyckoff, 1963), respectively; but they are in different oxidation states. As expected, the Cu $2p_{3/2}$ binding energy in Cu_2O is lower (932.5 eV) than in CuO (933.5 eV). Also, Figure 1a shows no shake-up lines for Cu in an oxidation state lower than 2 (Mosser *et al.*, 1991).

The different phyllosilicates (Table 2), as previously mentioned by other authors (Canesson, 1982), have the same Si 2p line position with a binding energy of 102.2–102.5 eV. This means that only one Si-O bonding type exists for all the studied phyllosilicates (Carrière and Deville, 1977), and the Si 2p line falls at the position of tetravalent silicon in the tetrahedral structural site of silica or silicates (Huntress and Wilson, 1972).

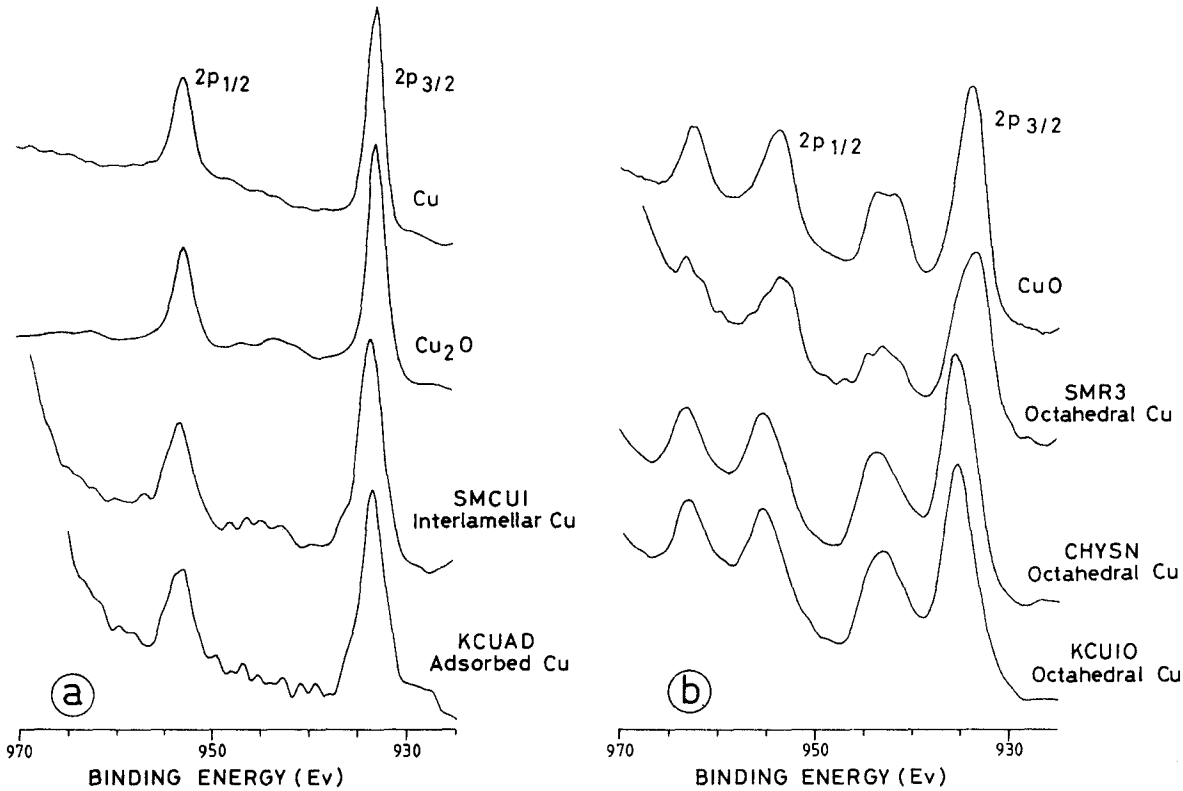

Figure 1. Cu $2p_{3/2}$ and Cu $2p_{1/2}$ XPS charge corrected spectra. SMCUI = smectite: Cu in interlamellar position; KCUAD = kaolinite: Cu on surface adsorbed position; SMR3 = synthetic smectite: Cu in octahedral position; CHYSN = chrysocolla: Cu in octahedral position; KCUOIO = synthetic kaolinite: Cu in octahedral position.

Table 2. Positions and widths for Cu $2p_{3/2}$, O 1s and Si 2p photoemission peaks.

Compounds	Cu $2p_{3/2}$		O 1s		Si 2p	
	BE(eV) (±0.2 eV)	FWHM (±0.05 eV)	BE(eV) (±0.2 eV)	FWHM (±0.05 eV)	BE(eV) (±0.2eV)	FWHM (±0.05eV)
Cu metal	932.5	2.04				
Cu_2O	932.5	2.20	530.1	2.54		
CuO	933.5	3.23				
Natural smectites						
SMBF (Si, Al, Fe, Cu, Sr)	935.3	2.69	532.2	2.46	102.5	2.20
SMCB (Si, Al, Mg, Fe)			531.8	2.57	102.2	2.36
SMCUI (Si, Al, Mg, Fe, Cu)	933.2	2.90	531.8	2.71	102.3	2.46
Synthetic smectites						
SMR3 (Si, Mg, Cu)	933.6	4.47	531.6	3.12	102.2	2.74
SMMG (Si, Mg)			532.1	2.82	102.5	2.45
Natural kaolinites						
KPA3 (Si, Al, Fe, Cu)	934.5	3.77	532.0	2.46	102.5	2.30
KMRX (Si, Al)			532.0	2.36	102.5	2.23
KCUAD (Si, Al, Cu)	933.4	2.90	531.9	2.46	102.5	2.31
Synthetic kaolinites						
KCUIO (Si, Al, Cu)	935.4	3.98	531.6	3.09	102.3	2.85
KCU7 (Si, Al, Cu)	935.1	—	531.7	2.80	102.3	2.60
Chrysocolla						
CHYSN (Si, Cu)	935.4	4.19	531.9	2.68	102.4	2.65
Gel for synthetic kaolinite						
CUIOCD (Si, Al, Cu)	935.7	4.62	531.7	3.32	102.2	2.83

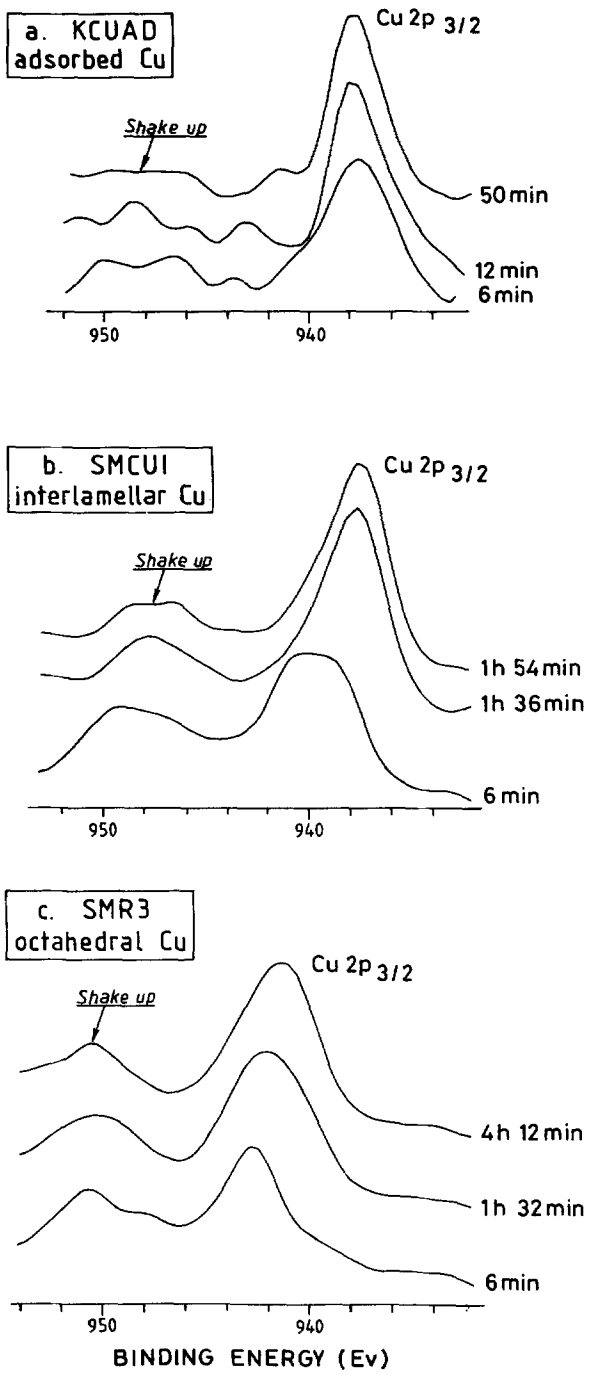

Figure 2. Photoreduction effects on Cu $2p_{3/2}$ XPS (uncorrected spectra) collected after varying lengths of exposure to X-ray beam.

Photoreduction effect

After 1 hr of X-ray irradiation of the samples, the Cu 2p photopeaks, by comparison with the oxide reference spectra, divide the phyllosilicate samples into two sets. In the first set (Figure 1a) are the minerals with adsorbed or interlamellar Cu whose spectra lack shake-up lines and are similar to that of the Cu(I) state in Cu_2O. The second set (Figure 1b) is comprised of the minerals with Cu in octahedral sites whose spectra contain shake-up lines as observed in CuO. The binding energy of the Cu $2p_{3/2}$ line for Cu in octahedral sites is higher (935.4 to 935.1 eV) than in adsorbed and interlamellar positions (933.2 and 933.4 eV).

Nevertheless, Cu in all phyllosilicates studied here was in the (II) oxidation state, as checked by ESR spectra (Creach, 1988; Mosser *et al.*, 1990a, 1990b). Koppelman and Dillard (1977) mentioned the reduction of Cu(II) adsorbed on chlorite by the photoreduction effect; this effect increased with exposure time to the X-ray beam. This phenomenon was also observed in other Cu(II) systems by Rosencwaig *et al.* (1971), Frost *et al.* (1972), and Wallbank *et al.* (1973).

The similarity of the photoelectron Cu 2p spectra of the phyllosilicates containing adsorbed or interlamellar Cu(II) with that of Cu_2O can be explained by the photoreduction effect. Synthetic Cu smectite SMR3 (Figure 1b) shows an asymmetric Cu $2p_{3/2}$ line with a shoulder at 935.1 eV, nearly the same position as in chrysocolla and the synthetic kaolinite with Cu in octahedral sites, however, the main Cu $2p_{3/2}$ position is at a lower energy (933.6 eV). The lower peak position is probably also due to the photoreduction effect.

The photoreduction effect has been evaluated on our samples by measuring XPS spectra at the very beginning of the X-ray exposure, then at various intervals during the 4-hr exposure. Each measurement lasted 6 minutes. These photoreduction experiments were performed on Cu(II) in the adsorbed position on kaolinite (KCUAD) (Figure 2a), on Cu(II) in the interlayer position of smectite (SMCUI) (Figure 2b), and on Cu(II) in the octahedral position of synthetic Cu smectite (SMR3) (Figure 2c). The C 1s line was not measured during the photoreduction experiment so the spectra are presented without charge correction. Binding energies for the Cu $2p_{3/2}$ peaks from some samples are also given (Table 3) without charge correction. The difference in binding energy between the Cu $2p_{3/2}$ and O 1s peaks, denoted ΔBE (Cu $2p_{3/2}$ − O 1s) in Table 3, was calculated to eliminate charge effects. Measurements on natural smectite (SMBF) and kaolinite (KPA3) samples with Cu in octahedral positions are also given in Table 3. All of these results show that when photoreduction occurs in the different samples it takes place at varying rates.

Adsorbed Cu. After 6 min of X-ray irradiation of the Cu-adsorbed kaolinite, we observed an asymmetric Cu $2p_{3/2}$ peak (940.9–937.5 eV charge not corrected). The higher binding-energy contribution is interpreted as the non-photoreduced part of the peak. After 12 min, the whole peak was displaced towards lower binding energy (ΔBE becomes smaller; Table 3) and the shake-

up peak corresponding to the Cu $2p_{3/2}$ peak was nearly absent (Figure 2a). All of these peaks remain stable when photoreduction occurs. Photoreduction apparently was achieved within 50 minutes, after which time the shake-up peak was no longer visible (Figure 2a).

Interlamellar Cu. After 6 min of X-ray irradiation of the smectite with Cu in the interlamellar position (SMCUI), we observed (Figure 2b) a broad Cu $2p_{3/2}$ peak (940.5–939.1 eV charge not corrected). After 96 min, the peak shifted towards lower binding energy where it seemed to stabilize. At the same time, the FWHM of the peak (Table 3) diminished from 5.3 eV to 3.7 eV and the Cu $2p_{3/2}$ shake-up peak nearly disappeared. Photoreduction apparently was complete after 96 min of irradiation (Figure 2).

Octahedral Cu. The natural smectite (SMBF) and kaolinite (KPA3), with Cu in octahedral positions, revealed no shift of the Cu $2p_{3/2}$ peak after 3 hr irradiation and thus no photoreduction effect.

On the other hand, sample SMR3 (a synthetic smectite) with Cu also in octahedral positions, presented a shift of part of the Cu $2p_{3/2}$ peak towards lower binding energy after 96 min of X-ray irradiation (Figure 2c). After 4 hr, the peak still remained asymmetric; the main peak was displaced to 941.3 eV (charge not corrected) with a shoulder remaining at higher energy (942.7 eV charge not corrected). The Cu $2p_{3/2}$ corresponding shake-up peak seemed to be stable or only slightly weakened (Figure 2c). Some photoreduction happened but it was much less than for Cu in interlamellar or adsorbed positions. The difference between natural and synthetic minerals can be explained by the fact that the natural smectites are better crystallized than the synthetic one. The crystal size, or coherency domain, in the ab-plane (using the Scherrer equation applied to the (060) X-ray reflection) is about 40 Å for the synthetic Cu smectite SMR3, about 150 Å for the natural smectite SMBF, and 400 Å for the natural kaolinite KPA3. The small size of the coherency domains and probable defects in the octahedral sheet of the synthetic Cu-smectite (Mosser *et al.*, 1990a) make Cu in the octahedral position sensitive to photoreduction, whereas octahedral Cu in well-crystallized phyllosilicates is insensitive to photoreduction.

These tests show that photoreduction takes place very quickly (less than 10 min), and is achieved within 50 min when Cu is adsorbed on the surface of the phyllosilicates. Almost twice that time is required for completed photoreduction in the interlamellar positions; it does not take place with Cu in octahedral sites of the natural phyllosilicates. Some photoreduction was observed in the synthetic Cu smectite.

Influence of crystallization

The synthetic Cu-kaolinite (KCUIO) and the gel (CUIOD) utilised for its synthesis are of the same chemical composition. CUIOD is amorphous and KCUIO is the crystallized product. The binding energies for Cu 2p, O 1s, and Si 2p are the same for the two products (Table 2), thus these three elements are in the same oxidation state and the same structural site in the gel and in the kaolinite. On the other hand, the Cu 2p and O 1s line widths (Table 2) of the crystallized product (3.98 eV and 3.09 eV, respectively) are smaller than for the gel (4.62 eV and 3.32 eV, respectively), whereas those of Si 2p are the same (2.85 and 2.83 eV, respectively).

Several authors (Onorato *et al.*, 1985; Hochella and Brown, 1988) pointed out, for glass systems and silicate minerals, that the O 1s FWHM depends on the proportion of bridging to non-bridging oxygens. This means that FWHM is sensitive to the geometrical arrangement of the (O, Si) tetrahedra in a silicate structure. Consequently, this parameter is also expected to be sensitive to the geometrical arrangement of the (O, cation) octahedra containing Cu cations.

Our experimental results can, therefore, be interpreted as follows. The geometrical arrangement of Cu octahedra is different in the crystallized and amorphous products, whereas it is the same for the Si tetrahedra. Thus, the relative proportions of bridging and non-bridging oxygens must be different between the crystallized and amorphous products. This is consis-

Table 3. Photoreduction effects on Cu $2p_{3/2}$ spectra.

Time of spectra acquisition (min)	Cu $2p_{3/2}$ BE eV (±0.2 eV)	Cu $2p_{3/2}$ FWHM eV (±0.05 eV)	ΔBE eV (Cu 2p-O 1s)
Natural smectite with Cu in octahedral positions (SMBF)			
6[1]	935.5	3.07	402.9
191[1]	935.3	2.69	403.1
Natural kaolinite with Cu in octahedral positions (KPA3)			
6[1]	935.0	4.28	402.6
191[1]	934.5	3.77	402.5
Synthetic Cu smectite with Cu in octahedral positions (SMR3)			
6	942.7	3.73	403.2
12	942.9	3.73	403.4
62[1]	933.6	4.47	402.0
92	942.0	4.00	402.5
252	941.3	3.87	401.8
Interlamellar Cu smectite (SMCUI)			
6	940.5–939.1	5.33	403.9–402.5
12	939.5	5.33	403.2
62[1]	933.2	2.90	401.4
96	937.6	3.73	401.9
114	937.4	3.73	401.7
Kaolinite Cu adsorbed (KCUAD)			
6	940.9–937.5	3.90	404.6–401.2
12	937.9	3.20	401.6
50	937.8	3.10	401.1
66	937.8	4.00	401.1
192[1]	933.4	2.90	401.5

[1] C1s charge corrected spectra.

Table 4. Position and width of photoemission peaks.

Compounds	O 1s		Si 2p		Al 2p	
	BE(eV) (±0.2 eV)	FWHM (±0.05 eV)	BE(eV) (±0.2 eV)	FWHM (±0.05 eV)	BE(eV) (±0.2 eV)	FWHM (±0.05 eV)
KMRX (Si, Al)	532.0	2.36	102.5	2.23	74.1	2.08
KCUAD (Si, Al, Cu)	531.9	2.46	102.5	2.31	74.2	2.15
SMCB (Si, Al, Mg, Fe)	531.8	2.57	102.2	2.36	74.2	2.29
SMCUI (Si, Al, Mg, Fe, Cu)	531.8	2.71	102.3	2.46	74.4	2.39
SMMG (Si, Mg)	532.1	2.82	102.5	2.45	50.0	2.46
SMR3 (Si, Mg, Cu)	531.6	3.12	102.2	2.74	49.6	2.80
CHYSN (Si, Cu)	531.9	2.68	102.4	2.65		
KCUIO (Si, Cu, Al)	531.6	3.09	102.3	2.85		

tent with the observed difference between the two O 1s FWHM. Also, the geometrical arrangement of the (Si,O) tetrahedra is a bi-dimensional arrangement of Si tetrahedra in the gel as in the clay structure, whereas Cu is in independent, non-bi-dimensionally arranged octahedra.

Influence of the chemical environment

Nature of cations. Three phyllosilicates with only Si in the tetrahedral sheet and containing different octahedral cations—Al in KMRX, Cu in CHYSN, and Mg in SMMG—were analysed. After synthesis about 10–20% amorphous product remained in the SMMG sample.

The binding energies of O 1s and Si 2p are about the same for the three phyllosilicates (Table 2), but the FWHM of Si 2p decreases in the order CHYSN > SMMG > KMRX. Cu broadens the Si 2p line (2.65 eV) more than does Mg (2.45 eV), which broadens the line more than Al (2.23 eV). FWHM of O 1s differs also with the nature of the octahedral cations, but decreases from SMMG > CHYSN > KMRX.

These observations indicate that O 1s FWHM is enlarged in amorphous material, whereas Si 2p FWHM is unaffected. Thus, part of the broadening of the SMMG O 1s line attributed to the presence of 10–20% gel. Taking this into account we can conclude that octahedral cations broaden the Si 2p and O 1s lines in the order Cu > Mg > Al.

Number and amount of cations. Table 4 lists the XPS peak parameters for samples paired according to like chemical composition. The second member of each pair (Table 4) differs from the first by only one cation. The binding energies of the several peaks are constant within experimental error of ±0.2 eV. However the widths of the O 1s, Si 2p, Al 2p, and Mg 2p lines are larger for the samples with the additional cation.

A positive correlation also exists between the broadening of the Si 2p, O 1s, and Al 2p peaks and the amount of additional cation present (Table 4). Three of the pairs differ by the presence of variable quantities of Cu: 1% in KMRX and KCUAD, 3.6% in SMBC and SMCUI, and 6% in SMMG and SMR3. The broadenings of their Si 2p lines are, respectively, 0.10, 0.14, and 0.30 eV; of their O 1s lines, 0.08, 0.10, and 0.29 eV; and of their Al 2p lines, 0.07, 0.10, and 0.34 eV.

CONCLUSIONS

In a previous paper, Mosser *et al.* (1990a) showed that ESR spectroscopy can distinguish Cu in octahedral sites from either interlamellar or adsorbed positions, but it is unable to differentiate interlamellar from surface adsorbed species. Results from the present study clearly demonstrate that, because of the photoreduction effect, XPS spectroscopy can distinguish octahedral from interlamellar, and interlamellar from adsorbed positions of Cu in clay minerals.

The different measurements which have been made show that XPS signals are sensitive to numerous crystallochemical parameters linked to local ordering around the probe cations. These parameters concern the nature, number, and amounts of cations, as well as the crystallinity of the analysed material. The "crystallinity" of phyllosilicates has no effect on the width (FWHM) of the Si 2p line (tetrahedral cation); only the O 1s and Cu 2p (octahedral cation) lines are affected. The chemical environment (nature, number, and amount of cations), however, affects the widths of all lines, including those of both the tetrahedral and octahedral sheets.

This type of analytical approach is indispensable for obtaining complete information on Cu geochemistry and metallogeny, particularly as it relates to Cu mobility. Cu is unleachable when located in octahedral positions, but is susceptible to mobilization when in the interlamellar position, and even more so in surface adsorbed positions.

REFERENCES

Asbrink, S., and Norrby, L. J. (1970) A refinement of the crystal structure of copper(II) oxide with a discussion of some exceptional E.s.d.'s: *Acta Cryst.* **B26, 8,** 8–15.

Canesson, P. (1982) E.S.C.A. studies of clay minerals: *Dev. Sedimentol.* **34** (Adv. Tech. Clay Miner. Anal.), J. J. Fripiat, ed., 211–226.

Carrière, B., and Deville, J. P. (1977) X-ray photoelectron study of some silicon-oxygen compounds: *J. Electron Spectrosc. Relat. Phenom.* **10,** 85–91.

Creach, M. (1988) Accumulation supergène de cuivre en milieu latéritique: Étude pétrologique, cristallochimique et géochimique de l'altération du skarn de Santa Blandina (Itapeva, Bresil): Thèse Doct., Univ. Poitiers, France, 124 pp.

Decarreau, A. (1985) Partitioning of divalent transition element between octahedral sheet of trioctahedral smectites and water: *Geochim. Cosmochim. Acta* **49,** 1537–1544.

Frost, D. C., Ishitani, A., and McDowell, C. A. (1972) X-ray photoelectron spectroscopy for copper compounds: *Mol. Phys.* **24,** 861–877.

Hochella, M. F., and Brown, G. E., Jr. (1988) Aspects of silicate surface and bulk structure analysis using X-ray photoelectron spectroscopy (XPS): *Geochim. Cosmochim. Acta* **52,** 1641–1648.

Hochella, M. F., and Carim, A. H. (1988) A reassessment of electron escape depth in silicon and thermally grown silicon dioxide thin films: *Surface Sci. Lett.* **197,** L260–L268.

Huntress, W. T., and Wilson, L. (1972) An ESCA study of lunar and terrestrial materials: *Earth Planet. Sci. Lett.* **15,** 59–64.

Koppelman, M. H., and Dillard, J. D. (1977) A study of the adsorption of Ni(II) and Cu(II) by clay minerals: *Clays & Clay Minerals* **25,** 457–462.

Mosser, A., Romeo, M., Parlebas, J. C., Okada, K., and Kotani, A. (1991) Photoemission on 2p core levels of copper: An experimental and theoretical investigation of the reduction of copper monoxides: *Solid State Communication* **91, 8,** 641–644.

Mosser, C., Mestdagh, M., Decarreau, A., and Herbillon, A. (1990a) Spectroscopic (ESR, EXAFS) evidence of Cu for (Al-Mg) substitution in octahedral sheets of smectites: *Clay Miner.* **25,** 271–282.

Mosser, C., Petit, S., Parisot, J. C., Decarreau, A., and Mestdagh, M. (1990b) Evidence of Cu in octahedral layers of natural and synthetic kaolinites: *Chem. Geol.* **84,** 281–282.

Onorato, P. I. K., Alexander, M. N., Struck, C. W., Tasker, G. W., Uhlmann, D. R. (1985) Bridging and nonbridging oxygen atoms in alkali aluminosilicate glasses: *J. Am. Ceram. Soc.,* **68,** 6, C148–C150.

Petit, S. (1990) Etude cristallochimique de kaolinites ferrifères et cuprifères de synthèse (150–250°C): Thèse Doct., Univ. Poitiers, France, 237 p.

Rosencwaig, A., Wertheim, G. K., and Guggenheim, H. J. (1971) Origins of satellites on inner-shell photoelectron spectra: *Phys. Rev. Lett.* **27,** 479–481.

Seyama, H., and Soma, M. (1985) Bonding-state characterization of the constituent elements of silicate minerals by X-ray photoelectron spectroscopy: *J. Chem. Soc., Faraday Trans.* **1, 81 (2),** 485–495.

Seyama, H., and Soma, M. (1988) Application of X-ray photoelectron spectroscopy to the study of silicate minerals: in *Kokiritsu Kogai Kenkyusho Kenkyu Hokoku (Research Report from the National Institute for Environmental Studies, Japan)* **111,** 125 pp.

Siegbahn, K., Nording, C. N., Fahlman, A., Nordberg, R., Hamrin, K., Hedman, J., Johansson, G., Bermark, T., Karlsson, S. E., Lindgren, I., and Lindgren, B. (1967) *ESCA: Atomic, Molecular, and Solid State Structure Studied by Means of Electron Spectroscopy:* Almqvist and Wiksells, Uppsala.

Stucki, J. W., Roth, C. B., and Baitinger, W. E. (1976) Analysis of iron-bearing clay minerals by electron spectroscopy for chemical analysis (ESCA): *Clays & Clay Minerals* **24,** 289–292.

Urch, D. S., and Murphy, S. (1974) The relationship between bond lengths and orbital ionisation energies for a series of aluminosilicates: *J. of Electron Spectrosc. Relat. Phenom.,* **5,** 167–171.

Wallbank, B., Johnson, C. E., and Main, I. G. (1973) Multielectron satellites in core electron photoemission from 3d° ions in solids: *J. Phys.* **C, 6,** L493–L495.

Wyckoff, R. W. G. (1963) *Crystal Structures:* 2nd ed., **1,** Interscience publishers, John Wiley and Sons, New York, 467 pp.

(Received 23 March 1992, accepted 1 October 1992; Ms. 2203)